Supporting Information

Zhang et al. 10.1073/pnas.1100764108

SI Methods

Cell Lines and Patient Samples. MCF10A, SKBR3, MCF7, MDA231, MDA453, MDA436, MDA468, HCC38, hMEC-hTERT, and 293 cell lines were purchased from American Type Culture Collection. The LY2 cell line was a gift from Lawrence Berkeley National Laboratory (Berkeley, CA). Cells were grown in the indicated medium containing 1× penicillin/streptomycin. Media used were as follows. MCF10A, 45% DMEM, 45% F-12 Ham's, 5% horse serum, 2.5 mM L-glutamine, 20 ng/mL EGF, 10 μg/mL insulin, 500 ng/mL hydrocortisone, and 100 ng/mL cholera toxin; SKBR3, MDA453, MDA468, MDA436 and 293, DMEM with 10% FBS; MCF7, 45% DMEM, 45% F-12 Ham's, and 10% FBS; MDA-MB-231, Iscove DMEM with 10% FBS; LY2, modified Iscove modified Eagle medium with 5% FBS; HCC38, RPMI with 10% FBS; and hMEC-hTERT, MEM and F-12 mixture (1:1) supplemented with 1% FBS, 40 μg/mL BPE, 12.5 μg/mL EGF, 1 μg/mL insulin, 10 μg/mL transferrin, 100 μM phosphorylethanolamine, 100 μM ethanolamine, 1.25 μg/mL hydrocortisone, 15 nM sodium selenate, 50 μM ascorbic acid, 1 μg/mL cholera toxin, and 10 nM triiodothyronine. Deidentified patient-matched normal and breast cancer samples were obtained from the Oregon Health and Science University Cancer Pathology Shared Resource (institutional review board approval nos. 4918 and 2086). cDNA samples used in Fig. 3*A* and Fig. S6*B* were provided by one of the authors (D.C.).

Generation of Stable Cells. MCF10A-TR-Myc cells (MCF10A-Myc) were generated by infecting a 100-mm dish of MCF10A cells with a lentivirus (approximate multiplicity of infection of 10) encoding the tet-repressor, pLenti6/TR (Invitrogen), in 5 mL MCF10A modified media (MCF10A media with 5% defined FBS instead of horse serum) and 6 μg/mL Polybrene for 12 h. Media was changed to 10 mL modified media for 24 h. Cells were then split at a 1:10 dilution and maintained in modified media supplemented with 5 μg/mL Blasticidin (Invitrogen) for 10 d until distinct colonies formed. Six colonies were picked, expanded, and screened for their ability to suppress the expression of CMV-driven V5-tagged Axin1 expressed from Lenti/TO/V5-Dest-Axin1 by transient lentiviral infection. The best suppressing colony was then infected with lentivirus (approximate multiplicity of infection of 10) expressing V5-Myc, pLenti4/TO/V5-Dest-Myc, as described for the tet-repressor infection. Cells were selected in 5 μg/mL Blasticidin and 200 μg/mL Zeocin (Invitrogen) for 10 d until distinct colonies formed. Six colonies were picked, expanded, and screened for their ability to only express V5-Myc when treated with 1 μg/mL doxycycline. The best clone was then used for further experiments and continually maintained in modified media with 5 μg/mL Blasticidin and 200 μg/mL Zeocin. Stable MCF10A-Myc-shAxin1 or empty vector control cells were generated by transfecting MCF10A-TR-Myc cells with shRNA plasmid expressing shAxin1 (NM_003502.2–612s1c1 and NM_003502.2–2728s1c1; Sigma) or empty vector (Sigma) and selected in modified media with 5 μg/mL Blasticidin, 200 μg/mL Zeocin, and 5 μg/mL puromycin for colony growth.

Antibodies. c-Myc N262 (sc-764; Santa Cruz Biotechnology) 1:1,000, Axin1 (A0481; Sigma), Axin1 (C76H11; Cell Signaling), V5 (R-960–25; Invitrogen) c-Myc Y69 (ab32072, 1:1,000; Abcam), c-Myc C33 (SC-42 AC; Santa Cruz Biotechnology), c-Myc pT58 (used in Western analysis; Y011034, 1:1,000; Applied Biological Material), c-Myc phospho-Thr58 (used in immunofluorescence; A00242, 1:50; GenScript), monoclonal c-Myc pS62 (for Western analysis; E71-161, 1:1,000; BioAcademia). Generation of the polyclonal c-Myc S62 phospho-specific antibody used in immunofluorescence has been described previously (1) and was used at 1:25 dilution.

[^{35}S]Methionine Pulse/Chase Experiments. [^{35}S]Methionine pulse/chase experiments were done as described previously (2). Briefly, cells were pulse-labeled with [^{35}S]methionine/cysteine for 20 min, followed by chase in medium containing excess unlabeled methionine and cysteine. ^{35}S-Labeled c-Myc was immunoprecipitated from equal cell counts at each chase time point and visualized by SDS/PAGE autoradiography and quantified by PhosphorImager. Representative experiments are shown. The rate of degradation of endogenous c-Myc in each experiment for each breast cancer cell line as well as MCF10A was calculated relative to the starting time point set at 100% and graphed on a semilog graph. Best-fit exponential lines were drawn with Excel. c-Myc half-life was calculated from exponential line equations and the average half-life ± SD is shown for each cell type. Pulse-chase results shown here are representative of two or three independent experiments for each cell line.

Immunofluorescence and Quantification of Immunofluorescence Staining Intensity. Serial paraffin sections from patients with matched normal and tumor formalin-fixed tissues were incubated with the pS62 (1:25) or pT58 (1:50) c-Myc–specific antibody overnight at 4 °C followed by Alexa Fluor 594 donkey anti-rabbit IgG and mounted by using antifade containing DAPI. Matched normal and tumor sections were placed on the same slide and stained simultaneously or adjacent normal was present in the tumor block and thus on the same section. Images were taken with a Hamamatsu digital camera mounted on a fluorescence microscope, and exposure and magnification were not changed within a slide comparing normal and tumor. Immunofluorescence density was analyzed with Openlab 5.5 software. Specifically, representative pictures from the same or adjacent sections were taken of normal acini, DCIS, and invasive carcinoma cells from each patient. Epithelial cell fluorescence was quantified in these pictures using the Measure Density tool. A maximum of10 representative regions of interest (i.e., clusters of epithelial cells) were measured and averaged for each condition and graphed ±SD.

Cell Proliferation Assay. Cell proliferation assays were done with 80,000 SKBR3 cells in 60-mm dishes containing 4 mL of media. At 18 h after plating, IWR-1 or DMSO was added to cells at the indicated concentrations. Media with compound were changed every other day for 5 d, and cells were counted at the indicated times with a hemacytometer.

Soft Agar Assay. The bottom and top agar layers were 0.8% and 0.35% Nobel agar, respectively. For each MCF10A clone, 2×10^4 cells were plated in triplicate in a six-well plate. Culture medium with or without 1 μg/mL doxycycline on top of the agar was changed every 3 to 4 d. At 4 wk after plating, colonies were fixed and stained with 0.005% crystal violet in 50% methanol/50% PBS solution. Colonies that were in clusters of at least three cells in diameter were counted in 10 random microscopic fields. For SKBR3 soft agar assays, 2.5×10^4 cells were plated, and cell culture media with 20 mM IWR-1 or DMSO on top of the agar was changed every day. Colonies were visible by day 6 and were counted as described earlier.

ChIP. Cells were crosslinked with 1% formaldehyde for 10 min and lysed in 700 μL ChIP lysis buffer (0.1% SDS, 0.5% Triton X-100,

20 mM Tris-HCl, pH 8.1, and 150 mM NaCl). Cell lysates were sonicated six times (output, 3.5; 30% duty; 10 pulses) and then cleared by centrifugation. Cell lysates was precleared with protein A beads. IPs were performed with antibody overnight at 4 °C. Immunoprecipitates were washed six times with ChIP lysis buffer and twice with 1× Tris-EDTA and eluted from the beads with elution buffer (0.1 M $NaHCO_3$ and 1% SDS). Elution products were raised to 0.2 M NaCl and incubated at 65 °C overnight. For quantitative ChIP experiments, the internal GAPDH primers were used as a negative control.

ChIP Primers and Antibodies. For quantitative ChIP experiments, primers to the promoter regions of c-Myc target genes, as well as internal GAPDH primers, were used to amplify DNA. The internal GAPDH primers were used as a negative control. qPCR was used to measure signals in 1% of the input material, as well as each IP. Primers used were as follows: nucleolin, forward, TTGCGACGCGTACGAGCTGG; reverse, ACTCCGACTAGGGCCGATAC; and E2F2, forward, TCACCCCTCTGCCATTAAAGG; reverse, AGCAGTGTATTCCCCAGGCC. The percentage of input was then calculated for each IP (control IgG and specific) as the IP signal above the input signal by using the formula $100 \times 2^{(\text{input Ct} - \text{IP Ct})}$. Relative level of bound DNA was then graphed as the percent input of the specific IP relative to the percent input of the mock IgG control by using GraphPad Prism software. Antibodies used in ChIP were Myc (N262), HA-11(AbM), normal rabbit IgG (Santa Cruz Biotechnology), and normal mouse IgG (Santa Cruz Biotechnology).

qRT-PCR. RNA was isolated from breast cancer cell lines by using TRIzol reagent (Invitrogen). Isolated RNA was DNase I-treated and purified by using an RNeasy mini kit (Qiagen). cDNAs were made by using a High Capacity cDNA Reverse Transcription Kit (Applied Biosystems) with random primers. qRT-PCR analysis was done by using TaqMan primers. Primers used in quantitative RT-PCR were c-*MYC* (Hs00905030_m1), *18s* (Hs99999901_s1), total *AXIN1* (Hs00394718_m1), *AXIN1V1* (Hs00394723_m1), *AXIN1V2* (Hs01558063_m1), *ACTIN* (Hs99999903_m1), *axin1v1*, forward, CGTGTCGGACTTGGAACTCT; *axin1v2*, forward, CCAAGCAGAGGACAAAATCAC; and mouse *axin1r4* (used for both V1 and *V2*), AGCTCCCTTCTTGGTTAGC.

Statistics. SD was analyzed with Microsoft Excel, with results from three independent experiments unless otherwise indicated. *P* value was analyzed by Student *t* test. A two-tailed method was used unless otherwise indicated.

Generation of Transgenic Mice. RFS-Myc mice (3) were crossed with NeuNT (4) and MMTV-Cre or BLG-Cre mice (gift from Owen Sansom, Beatson Institute for Cancer Research, Glasgow, United Kingdom) to get mice that express both Myc and Neu in response to Cre-mediated recombination in the mammary gland. Mammary gland tumors were harvested and frozen for RNA analysis or embedded in paraffin for immunofluorescence staining.

1. Escamilla-Powers JR, Sears RC (2007) A conserved pathway that controls c-Myc protein stability through opposing phosphorylation events occurs in yeast. *J Biol Chem* 282: 5432–5442.
2. Malempati S, et al. (2006) Aberrant stabilization of c-Myc protein in some lymphoblastic leukemias. *Leukemia* 20:1572–1581.
3. Wang X, et al. (2011) Phosphorylation regulates c-Myc's oncogenic activity in the mammary gland. *Cancer Res* 71:925–936.
4. Andrechek ER, et al. (2000) Amplification of the neu/erbB-2 oncogene in a mouse model of mammary tumorigenesis. *Proc Natl Acad Sci USA* 97:3444–3449.

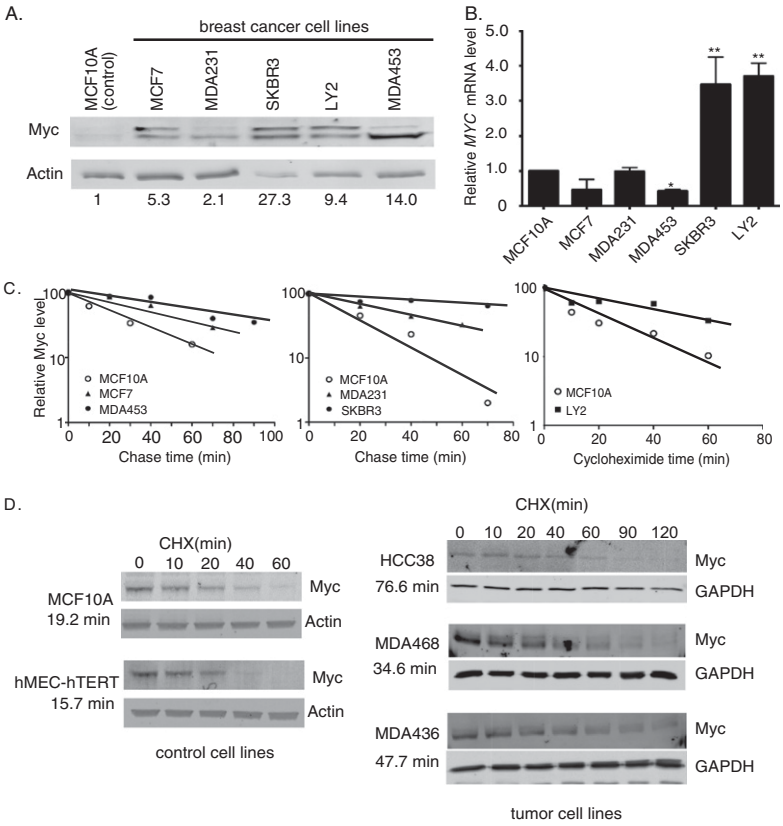

Fig. S1. Increased c-Myc protein stability contributes to c-Myc overexpression in human breast cancer cell lines. (*A*) Western analysis of c-Myc protein expression in human breast cancer cell lines. Representative Western blot is shown. Numbers below are the average fold change normalized to β-actin and relative to MCF10A. (*B*) Real-time qPCR analysis of c-*MYC* mRNA levels in breast cancer cell lines (**P <0.01, *P < 0.05). (*C*) The rate of c-Myc degradation for breast cancer and control cell lines is represented in the graph by best-fit exponential lines. c-Myc half-life was calculated from exponential line equations. (*D*) c-Myc half-life in control and breast cancer cell lines determined by cycloheximide treatment.

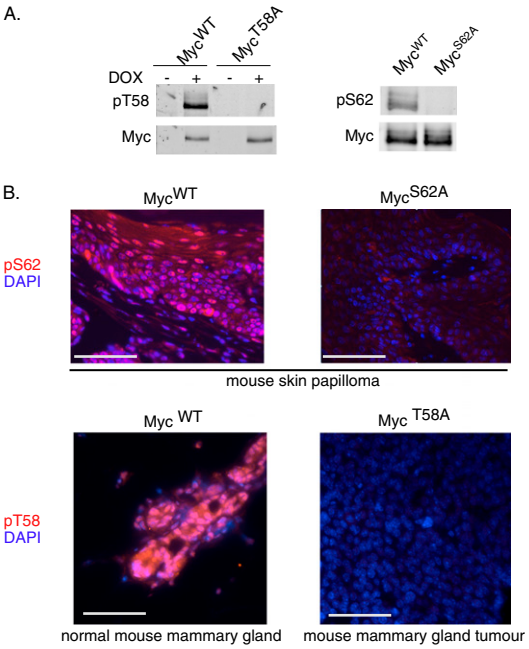

Fig. S2. Characterization of phospho–c-Myc antibodies used in Western blot and immunofluorescence staining. (*A*) Western blots showing antibody specificity. Protein lysates from MCF10A cells stably expressing doxycycline-inducible V5-tagged c-Myc^{WT}, c-Myc^{T58A}, or c-Myc^{S62A} were analyzed by Western blotting with the V5 antibody for total V5-tagged c-Myc (V5; Invitrogen), the pS62 antibody (E71-161; BioAcademia), or the pT58 antibody (Applied Biological Material) as indicated. Blots were dual-probed with phospho-Myc antibodies and the V5 antibody and imaged by using a LI-COR imager (*Methods*). (*B*) Specificity of pT58 and pS62 antibodies for immunofluorescence assays (IF) on formalin-fixed, paraffin-embedded tissue sections. Mouse tissues ectopically expressing c-Myc^{WT}, c-Myc^{T58A}, or c-Myc^{S62A} were formalin-fixed, paraffin-embedded and analyzed by IF as indicated. *Upper*: Mouse skin papilloma sections from our skin cancer model (DMBA/TPA), in which expression of c-Myc^{WT} (*Left*) or c-Myc^{S62A} (*Right*) was driven from the ROSA promoter in response to K5-Cre in epidermal skin cells, were stained with our rabbit polyclonal pS62 antibody (red) and DAPI (blue). Merged image is shown. pS62 staining was positive in c-Myc^{WT}–expressing papilloma, but negative in c-Myc^{S62A}–expressing papilloma. *Bottom*: Merged images of pT58 antibody (red; GenScript) and DAPI (blue) staining of normal mouse mammary gland ectopically expressing c-Myc^{WT} driven by the ROSA promoter in response to WAP-Cre (*Left*) and mammary gland tumor induced by expression of c-Myc^{T58A} driven in the same way (*Right*). c-Myc^{WT} in normal cells shows high pT58 levels as expected; c-Myc^{T58A} lacks phosphorylation at T58 and is negative for staining. Note that ectopic expression of c-Myc in these mouse models reduces expression of endogenous c-Myc. (Scale bars: 50 μM.)

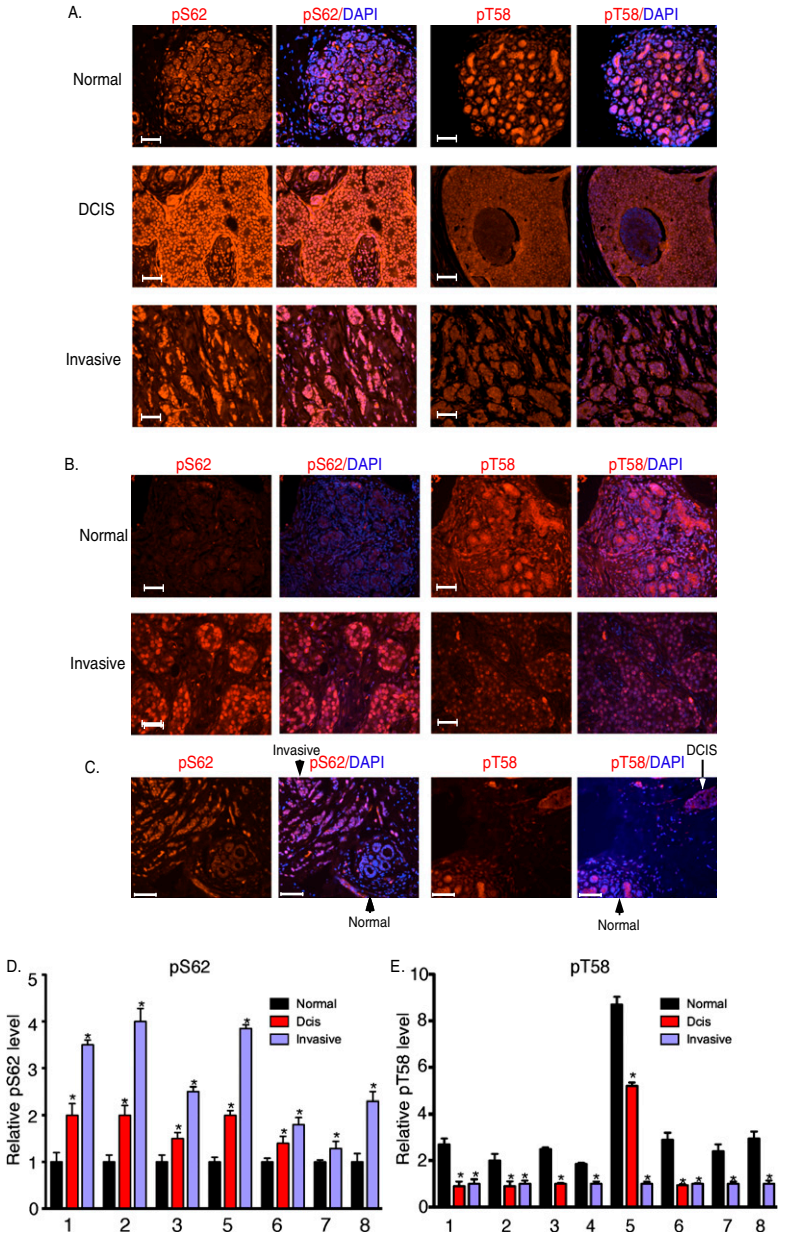

Fig. S3. Increased pS62 and decreased pT58 levels in human breast tumors compared with patient-matched normal breast tissue. (*A*) Patient-matched sections of tumor and normal tissue were placed on the same slide and stained with pS62- or pT58-specific antibody (red). Nuclei were counterstained with DAPI (blue). The right panel in each column is the merged phospho-Myc/DAPI image. For each antibody, all pictures were taken at the same exposure. Normal acini, regions of DCIS, and invasive adenocarcinoma from patient 6 are shown. (*B*) pS62 and pT58 staining of normal and invasive adenocarcinoma from patient 8. Immunofluorescence staining was done as in *A*. (*C*) pS62 and pT58 staining of adjacent normal and tumor cells from patient 6 in the same microscope field are shown. (Scale bars: 50 μM.). (*D*) pS62 staining density from seven patients was quantified as described in *Methods*, and averages ± SD were graphed relative to normal (note staining from patient 4 was not attainable in this set). Because of space limits, $*P < 0.001$ between DCIS or invasive carcinoma and normal samples. (*E*) Same as *D*, except showing pT58 staining density and including patient 4. Averages of pT58 levels ± SD were graphed relative to invasive carcinoma or DCIS, whichever was lower.

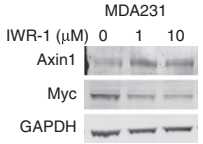

Fig. S4. IWR-1 decreases c-Myc expression in MDA231 cells. MDA231 cells were treated with IWR-1 at the indicated concentration for 24 h, and Axin1, c-Myc, and Actin expression was monitored by Western blotting.

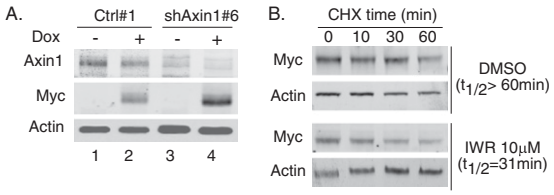

Fig. S5. Axin1 regulates c-Myc protein expression and stability. (*A*) MCF10A cells that express doxycycline-inducible c-Myc were transfected with empty vector (Ctrl) or shRNA against Axin1 and stable clones (Ctrl#1 and shAxin1#6) were selected and analyzed for expression of Axin1 and ectopic Myc with or without 1 μg/mL doxicycline (Dox) treatment for 24 h. (*B*) SKBR3 cells were treated with 10 μM IWR1 or DMSO for 4 h and then treated with cycloheximide (CHX) for the indicated times before harvesting for Western analysis. c-Myc half-life was determined as in Fig. 1*B* and Fig. S1*D*.

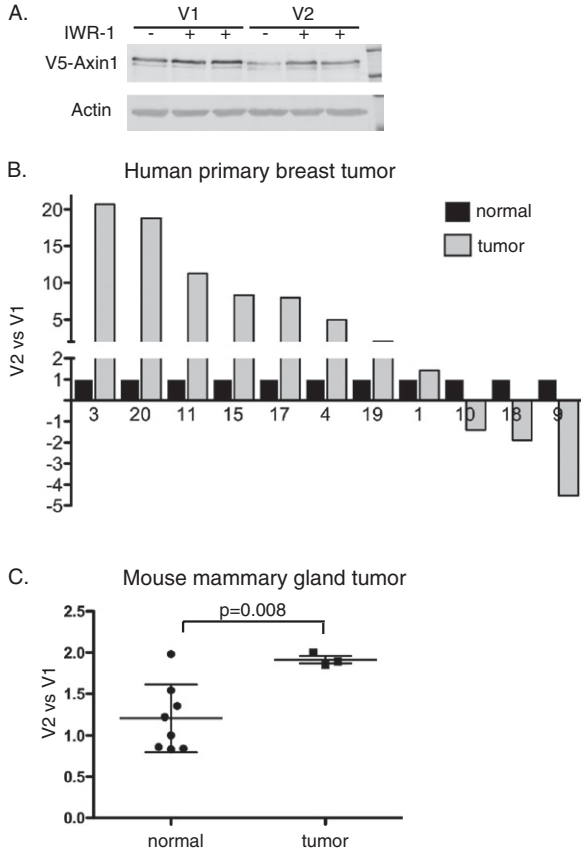

Fig. S6. Tumor cells have higher ratio of *AXIN1V2* versus *AXIN1V1* than normal cells. (*A*) SKBR3 cells were infected with lentivirus that expresses v5-tagged Axin1v1 or Axin1v2 for 24 h and then treated with DMSO or 10 μM IWR1 for another 24 h. Shown are Western blots of V5 antibody for Axin1 expression and loading control Actin. (*B*) qRT-PCR analysis of *AXIN1V1 and AXIN1V2* mRNA levels in human breast tumors. The ratio of *V2* versus *V1* in each tumor sample was graphed relative to its matched normal sample. The matched normal/tumor ratios were log-transformed and a *P* value for increased ratio was calculated by one-tailed Student *t* test ($P = 0.015$). (*C*) *axin1v1* and *axin1v2* expression was analyzed in normal mammary gland tissues by qRT-PCR and in mouse mammary tumors from our Cre-inducible, Rosa-Floxed-Stop (RFS)–Myc^{WT};MMTV or BLG-Cre;NeuNT mice. Myc^{WT} and Neu synergize in these mice for rapid tumorigenesis. The ratio of *v2* versus *v1* was set to 1 in one of the normal samples and the relative ratios of *v2* versus *v1* in the rest of the samples were calculated and graphed. The *P* value was calculated by using a one-tailed Student *t* test.

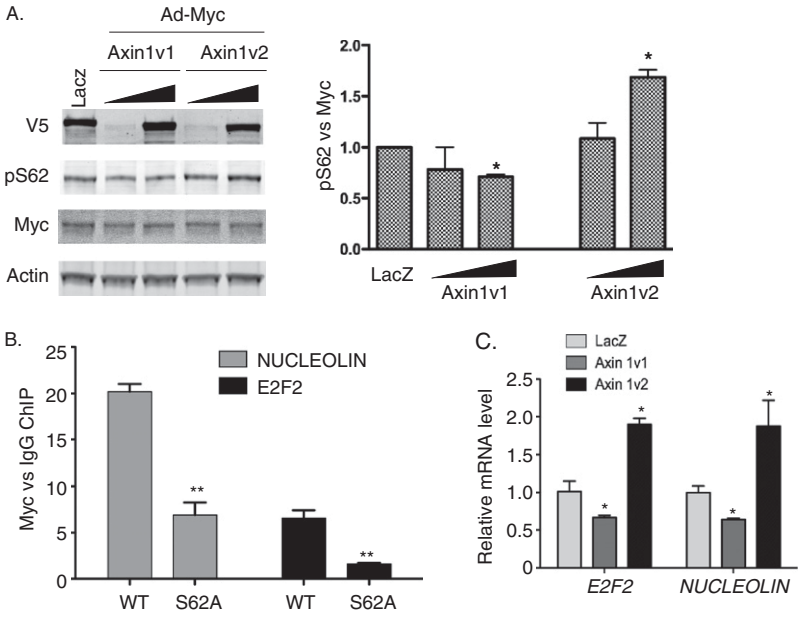

Fig. S7. Axin1v1 but not Axin1v2 decreases pS62-c-Myc and Myc function. (*A*) SNU475 cells were infected with lentivirus expressing control LacZ or one of the splice variants of Axin1 for 48 h, followed by infection with adenovirus expressing HA-tagged Myc. Western blot was done to analyze expression of Axin1, pS62, Myc, and Actin. pS62 versus Myc levels in Axin1v1- or Axin1v2-expressing cells were normalized to that of LacZ-expressing cells, and results from two experiments were calculated and graphed (*$P < 0.05$). (*B*) MCF10A stable cell lines that express doxycycline inducible V5-tagged Myc^{WT} or Myc^{S62A} were treated with doxycycline for 24 h. ChIP experiment was done with V5 antibody, and the amount of V5 bound *NUCLEOLIN* and *E2F2* was normalized to IgG-bound ones and graphed (**$P < 0.01$). (*C*) SNU475 cells were infected as in Fig. 5*E*. *E2F2* and *NUCLEOLIN* mRNA expression were analyzed by qRT-PCR and graphed relative to *GAPDH* ± SD (*$P < 0.05$).

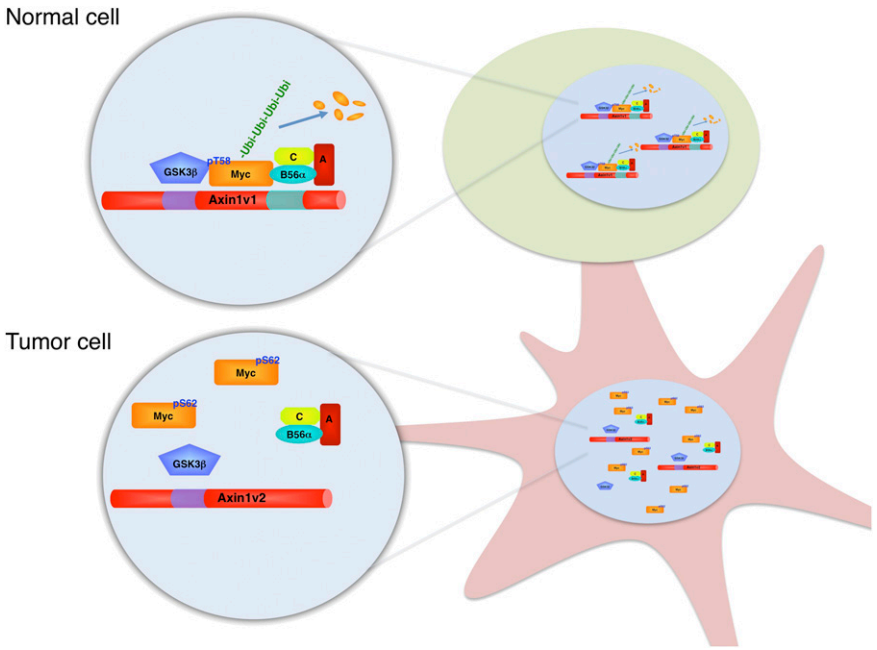

Fig. S8. Model showing deregulation of Axin1 and c-Myc protein degradation in cancer cells. In normal cells, c-Myc is recruited to a destruction complex coordinated by the Axin1 scaffold protein containing GSK3β, PP2A, and other proteins (not included here). GSK3β phosphorylates c-Myc at T58, which triggers dephosphorylation at S62 by PP2A and its subsequent polyubiquitination by the SCF^{Fbw7} E3 ubiquitin ligase that targets it for proteasomal degradation. This can occur in the nucleus, and Axin1 can be detected at the promoters of Myc target genes (1). In tumor cells, deregulation of Axin1 caused by decreased total Axin1 levels and/or the switch to Axin1v2 and loss of the domain implicated in PP2A binding leads to disruption of the c-Myc degradation complex. As a result, c-Myc accumulates in the nucleus with high S62 phosphorylation.

1. Arnold HK, et al. (2009) The Axin1 scaffold protein promotes formation of a degradation complex for c-Myc. *EMBO J* 28:500–512.

Table S1. Summary of human breast ductal invasive carcinomas in this study and their pS62 staining intensity

Case	ER, PR, Her2 status	Grade	Stage	pS62 intensity*
1	ND	ND	ND	+++
2	$ER^+PR^+Her2^-$	II	T3N2	+++
3	$ER^+PR^+Her2^-$	III	T1N2	+++
4	$ER^-PR^-Her2^+$	II	T2N1	+++
5	ER^+PR^+Her2-	III	T1N2	+++
6	$ER^-PR^-Her2^-$	III	T3N3	+++
7	$ER^-PR^-Her2^-$	III	T3N3	+++
8	$ER^+PR^+Her2^-$	I	T1N2	++
9	$ER^-PR^-Her2^-$	II	T3N3	++
10	$ER^-PR^-Her2^+$	III	T3N3	++
11	$ER^+PR^+Her2^-$	I	T1N2	++
12	$ER^+PR^+Her2^-$	III	T3N2	++
13	$ER^+PR^+Her2^-$	I	T2N0	++
14	$ER^-PR^-Her2^+$	II	T3N2	++
15	$ER^+PR^+Her2^-$	III	T2N0	+
16	$ER^+PR^+Her2^-$	III	T3N2	+
17	$ER^-PR^-Her2^+$	II	T3N2	0
18	$ER^-PR^-Her2^+$	III	T2N3	–
19	$ER^-PR^-Her2^-$	III	ND	–
20	$ER^-PR^-Her2^+$	II	T3N2	—
21	$ER^-PR^-Her2^-$	III	T3N3	–
22	$ER^-PR^-Her2^-$	III	T4N3	–

Hormone receptor (ER/PR) status and Her2 status as well as stage and grade are indicated for the patient samples used in this study. The information was obtained from the pathology laboratory of Oregon Health and Science University in collaboration with one of the authors (M.T.). The pS62 immunofluorescence intensity in each tumor and its matched normal tissue was obtained as described in *Methods*. The relative pS62 intensity in each tumor was then calculated by normalizing to its matched normal tissue. pS62 intensity is summarized as follows: +, 1–1.5; ++, 1.5 ≤ 2; +++, >2; 0, no difference; –, 0.5–1; —, <0.5. ND, not determined.

*We cannot rule out the possibility that technical issues such as differences in fixation or embedding during sample preparation might affect the immunofluorescence intensity between matched normal and tumor.

Table S2. Summary of pS62 staining intensity in Myc/Neu-driven mouse mammary gland tumors

Sample	pS62 intensity
Tumor 1	++
Tumor 2	++
Tumor 3	+++
Normal	1

Three mammary gland tumors were collected from mice that express both Myc and Neu in the mammary gland. Two normal mammary glands were collected from WT mice. Normal and tumor tissues were formalin fixed and embedded in paraffin, cut, and subject to pS62 staining. Immunofluorescence were done and quantified as in Fig. 2. Average pS62 intensity in the two normal mouse mammary glands was set to 1 and relative pS62 intensity in tumors was calculated and summarized as follows: ++, 1.5 ≤ 2; +++, >2.